

See discussions, stats, and author profiles for this publication at: <https://www.researchgate.net/publication/231205883>

# Characterization of a Single Sample by Combining Thermodynamic and Spectroscopic Information in Spectral Analysis

ARTICLE *in* ANALYTICAL CHEMISTRY · MAY 1996

Impact Factor: 5.64 · DOI: 10.1021/ac951147p

---

CITATIONS

43

---

READS

35

3 AUTHORS, INCLUDING:



Mikael Kubista

Independent Researcher

176 PUBLICATIONS 10,400 CITATIONS

SEE PROFILE

# Characterization of a Single Sample by Combining Thermodynamic and Spectroscopic Information in Spectral Analysis

Jan Nygren,<sup>†</sup> José Manuel Andrade,<sup>‡</sup> and Mikael Kubista<sup>\*,†</sup>

Molecular Biotechnology Group, Department of Biochemistry and Biophysics, Chalmers University of Technology, S-413 90 Göteborg, Sweden, and Department of Analytical Chemistry, University of A Coruña, A Coruña, Spain

**We have previously shown that chemical equilibria can be characterized spectroscopically, even when the component spectral responses are unknown and overlapping, by exploiting appropriate thermodynamic relations (Kubista, M.; Sjöback, R.; Albinsson, B. *Anal. Chem.* 1993, 65, 994–998). Application of this strategy requires sets of samples that differ in a physical property, such as pH or total concentration. In this work, we show that a similar strategy can be applied to characterize a single sample. Utilizing the van't Hoff relation, which describes the dependence of the equilibrium constant on temperature, we show that spectra recorded at different temperatures can be deconvoluted into contributions from the individual components. To illustrate the approach, we characterize two monomer/dimer equilibria, thiazole orange in aqueous solution and benzoic acid in *n*-heptane, by studying the effect of temperature on the absorption spectrum. We determine the spectral responses of the monomer and dimer species, their concentrations as a function of temperature, and the enthalpy change upon dimerization. These are the first examples ever where the spectral responses of the components in a single sample are determined without making assumptions about spectral overlap and without reference spectra.**

The resolving power of spectroscopic methods is usually sufficient to separate the responses of the different components in a sample so their concentrations can be quantified. If the component spectra overlap, the concentrations are usually determined by comparison with appropriate references.<sup>1</sup> Without reference samples, the situation becomes complicated. Already in their pioneer work, Lawton and Sylvestre showed that not even a two-component system can be analyzed unambiguously.<sup>2</sup> Using the criteria of nonnegative concentrations and nonnegative spectral responses, they showed that the number of possible solutions could be limited. These assumptions are not always warranted owing to experimental noise; even when they are justified, the allowed range is usually unacceptably large for quantitative purposes. Systems with more than two components are complicated to analyze this way.<sup>3</sup>

Recently we developed two approaches that provide the accessory information that eliminates the solution degeneracy. In the first approach, constraining information is obtained by recording two different kinds of spectra on each sample that provide suitably correlated spectral responses.<sup>4,5</sup> The combined spectral information is then sufficient to uniquely determine both the spectral responses and the concentrations of the components. The second approach is applicable when the components are in chemical equilibrium. Samples that differ in a physical property, such as pH or sample concentration, can then be analyzed using the functional form of the equilibrium as a constraint to calculate the equilibrium constant, the component concentrations, and their spectral responses.<sup>6,7</sup> Common to these approaches is that they require a series of samples that contain the same components at different relative concentrations. So far, no method has been available to characterize both the spectral responses and the concentrations of the components in a single sample.

In the second approach, component concentrations are altered by changing the sample composition, and in the analysis it is assumed that this does not affect the equilibrium constant. In this work we show that, by changing a physical property instead, which alters the equilibrium constant in a predictable way, it is possible to characterize a single sample containing components in chemical equilibrium. We demonstrate this novel approach with two examples. First, we study the effect of temperature on the absorption spectrum of the dye thiazole orange using the thermodynamically predicted temperature dependence of the equilibrium constant as a constraint. We determine the thiazole orange monomer and dimer spectra, their concentrations as a function of temperature, and the change in enthalpy,  $\Delta H^\circ$ , and entropy,  $\Delta S^\circ$ , of the reaction. As a second example, we study the already thoroughly characterized monomer/dimer equilibrium of benzoic acid in *n*-heptane and compare our results with those of previous determinations.<sup>6,8</sup>

## MATERIALS AND METHODS

Thiazole orange was synthesized as described,<sup>9</sup> and its purity was checked spectroscopically. Benzoic acid and *n*-heptane were purchased from Merck. Absorption spectra were measured in a 1 cm cell on a CARY 4 spectrometer using 1 nm slit width, and

<sup>†</sup> Chalmers University of Technology.

<sup>‡</sup> University of A Coruña.

(1) Sánchez, E.; Kowalski, B. R. *Anal. Chem.* **1986**, 58, 496–499.

(2) Lawton, W. H.; Sylvestre, E. A. *Technometrics* **1971**, 13, 617–633.

(3) Borgen, O.; Davidsen, N.; Mingyang, Z.; Øyen, Ø. *Microchim. Acta* **1986**, 2, 63–67.

(4) Kubista, M. *Chemom. Intell. Lab. Syst.* **1990**, 7, 273–279.

(5) Scarminio, I.; Kubista, M. *Anal. Chem.* **1993**, 65, 409–416.

(6) Kubista, M.; Sjöback, R.; Albinsson, B. *Anal. Chem.* **1993**, 65, 994–998.

(7) Kubista, M.; Sjöback, R.; Nygren, J. *Anal. Chim. Acta* **1995**, 302, 121–125.

(8) Hosoya, H.; Tanaka, J.; Nagakura, S. *J. Mol. Spectrosc.* **1962**, 8, 257–275.

(9) Brooker, L. G. S.; Sprague, R. H.; Cressman, H. W. *J. Am. Chem. Soc.* **1945**, 67, 1889–1893.

spectra were digitized with five data points per nanometer. They are presented in molar absorptivities assuming 55 000 M<sup>-1</sup> cm<sup>-1</sup> at 500 nm of the thiazole orange monomer and 12 000 M<sup>-1</sup> at 227 nm of the benzoic acid monomer. Prior to use, the cuvette cell was treated with repel-silane to prevent adsorption.

## THEORY

Spectra recorded at different temperatures are arranged as rows in an  $n \times m$  matrix **A**, where  $n$  is the number of spectra and  $m$  the number of data points in each spectrum. **A** is decomposed into an orthonormal basis set using, for example, NIPALS:<sup>7,10</sup>

$$\mathbf{A} = \mathbf{TP}' + \mathbf{E} \approx \mathbf{TP}' = \sum_{i=1}^r \mathbf{t}_i \mathbf{p}_i' \quad (1)$$

where  $\mathbf{t}_i$  ( $n \times 1$ ) are orthogonal target vectors and  $\mathbf{p}_i'$  ( $1 \times m$ ) are orthonormal projection vectors. These are mathematical constructs and do not correspond to any physical property of the system.  $r$  is the number of spectroscopically distinguishable components, and **E** is the error matrix containing experimental noise. For a well-designed experiment, **E** is small compared to **TP'** and can be discarded.

Assuming linear response the recorded spectra are also linear combinations of the spectral responses,  $\mathbf{v}_i$  ( $1 \times m$ ), of the components:

$$\mathbf{A} = \mathbf{CV} + \mathbf{E} \approx \mathbf{CV} = \sum_{i=1}^r \mathbf{c}_i \mathbf{v}_i \quad (2)$$

where  $\mathbf{c}_i$  ( $n \times 1$ ) are vectors containing the component concentrations at the different temperatures. The two equations are related by a rotation:<sup>6,7</sup>

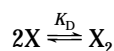
$$\mathbf{C} = \mathbf{TR}^{-1} \quad (3)$$

$$\mathbf{V} = \mathbf{RP}' \quad (4)$$

where **R** is an  $r \times r$  rotation matrix. For a two-component system,

$$\mathbf{R} = \begin{bmatrix} r_{11} & r_{12} \\ r_{21} & r_{22} \end{bmatrix} \quad \text{and} \quad \mathbf{R}^{-1} = \frac{1}{r_{11}r_{22} - r_{12}r_{21}} \begin{bmatrix} r_{22} & -r_{12} \\ -r_{21} & r_{11} \end{bmatrix} \quad (5)$$

Since a single sample is studied, the total concentration must be constant, constraining matrix **R**.<sup>11</sup> For a monomer/dimer equilibrium,



the total concentration of monomers is constant:

$$c_X(T) + 2c_{X_2}(T) = c_{\text{tot}} \quad \text{or} \quad \mathbf{c}_X + 2\mathbf{c}_{X_2} = \mathbf{c}_{\text{tot}} \quad (6)$$

Combining with eq 3, we obtain

(10) Fisher, R.; MacKenzie, W. J. *Agric. Sci.* **1923**, *13*, 311–320.

(11) Eriksson, S.; Kim, S. K.; Kubista, M.; Nordén, B. *Biochemistry* **1993**, *32*, 2987–2998.

$$\frac{1}{r_{11}r_{22} - r_{12}r_{21}}(\mathbf{t}_1 r_{22} - \mathbf{t}_2 r_{21} - 2\mathbf{t}_1 r_{12} + 2\mathbf{t}_2 r_{11}) = \mathbf{c}_{\text{tot}} \quad (7)$$

which can be written

$$f_{11}\mathbf{t}_1 + f_{12}\mathbf{t}_2 = \mathbf{c}_{\text{tot}} \quad (8)$$

where

$$f_{11} = (r_{22} - 2r_{12})(r_{11}r_{22} - r_{12}r_{21})^{-1} \quad (9)$$

and

$$f_{12} = (2r_{11} - r_{21})(r_{11}r_{22} - r_{12}r_{21})^{-1} \quad (10)$$

These can be determined, for example, by fitting the two target vectors to a vector with all elements equal to  $c_{\text{tot}}$ . Equations 9 and 10 provide two relations between the elements of matrix **R**, hence making two of them redundant.

In most cases, the spectra of some of the components can be determined in separate measurements. For example, a monomer/dimer equilibrium can, in general, be diluted sufficiently to make the dimer concentration negligible. This makes it possible to record the monomer spectrum, which, of course, should be used as a constraint in the analysis. Normalizing the monomer spectrum to the same total concentration as the analyzed sample, we obtain from eq 4

$$\mathbf{v}_{\text{monomer}} = r_{11}\mathbf{p}_1' + r_{12}\mathbf{p}_2' = f_{21}\mathbf{p}_1' + f_{22}\mathbf{p}_2' \quad (11)$$

where  $f_{21} = r_{11}$  and  $f_{22} = r_{12}$  are determined by fitting the two projection vectors to the monomer spectrum. Equation 11 also provides two relations between the elements of matrix **R**. These are not independent of eq 8, and the two equations cannot be combined to solve for all the elements of matrix **R**, but they can be used to express **R** in a single element, below arbitrarily chosen to be  $r_{21}$ :

$$\mathbf{R} = \begin{bmatrix} f_{21} & f_{22} \\ r_{21} & 2f_{22} + (2f_{21} - r_{21})\frac{f_{11}}{f_{12}} \end{bmatrix} \quad (12)$$

Defined this way, matrix **R** produces **C** and **V** matrices that are consistent with the total sample concentration and the spectral response of the monomer. The value of  $r_{21}$  determines the dimer spectrum and the monomer concentration profile. Although any value of  $r_{21}$  produces a mathematically acceptable solution, reasonable results, in terms of spectral intensities and nonnegative concentrations and spectral responses, are obtained in a relatively narrow range of  $r_{21}$  values. Still, the range is, in general, too large for a quantitative analysis.

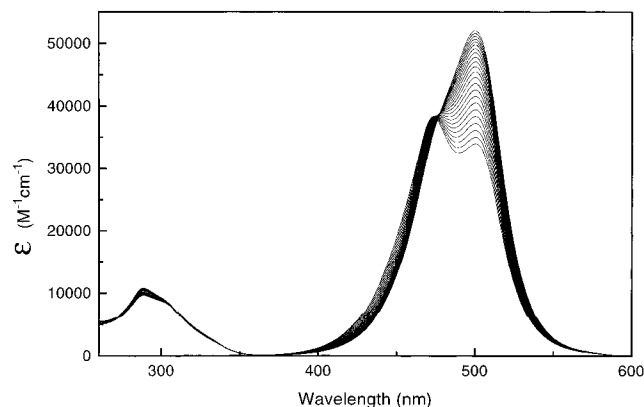


Figure 1. Absorption spectra of thiazole orange (36  $\mu\text{M}$ ) in water recorded at 2.5  $^{\circ}\text{C}$  intervals between 15  $^{\circ}\text{C}$  and 70  $^{\circ}\text{C}$ .

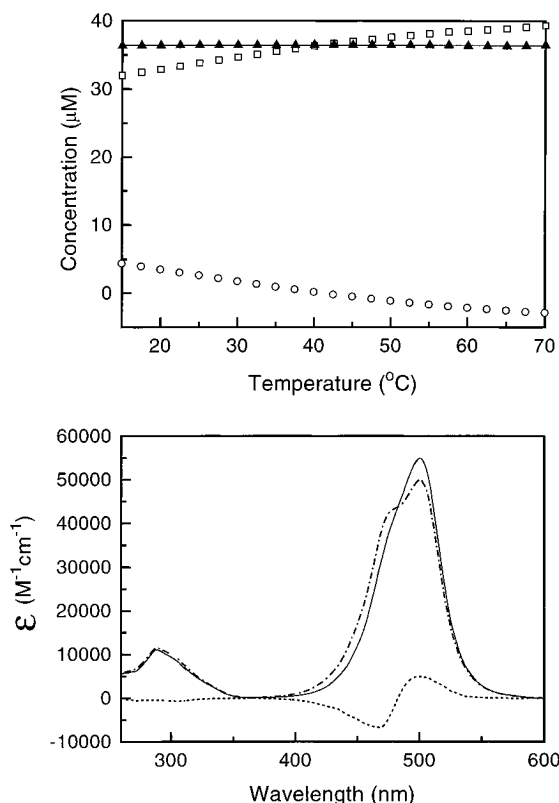


Figure 2. (Top) Scaled target vectors  $f_{11}\mathbf{t}_1$  ( $\square$ ),  $f_{12}\mathbf{t}_2$  ( $\circ$ ), and their sum ( $\blacktriangle$ ) compared to  $c_{\text{tot}}$  (—). (Bottom) Scaled projection vectors  $f_{21}\mathbf{p}_1$  (---) and  $f_{22}\mathbf{p}_2$  (- - -). Their sum fits perfectly to a spectrum of thiazole orange monomer (—).

The final constraint, which produces a unique solution, is the thermodynamic relation between temperature and the equilibrium constant. The components' concentrations are related by the law of mass action:<sup>12</sup>

$$K_D(T) = \frac{c_X(T)/c^\circ}{(c_X(T)/c^\circ)^2} \quad (13)$$

where  $c^\circ \equiv 1 \text{ mol/dm}^3$ . Assuming that the dimerization constant  $K_D(T)$  depends on temperature according to the van't Hoff equation,<sup>13</sup>

(12) Levine, I. N. *Physical Chemistry*, 3rd ed.; McGraw-Hill Book Co.: Singapore, 1988; Section 6.2.

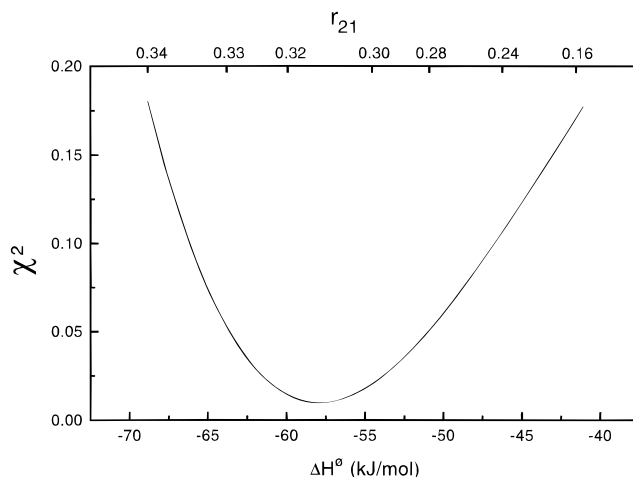


Figure 3. Plot of  $\chi^2$  of the linear regression of  $\ln K_D$  with respect to  $1/T$ , as a function of  $\Delta H^\circ$ . The corresponding  $r_{21}$  values are shown in the top x-axis.

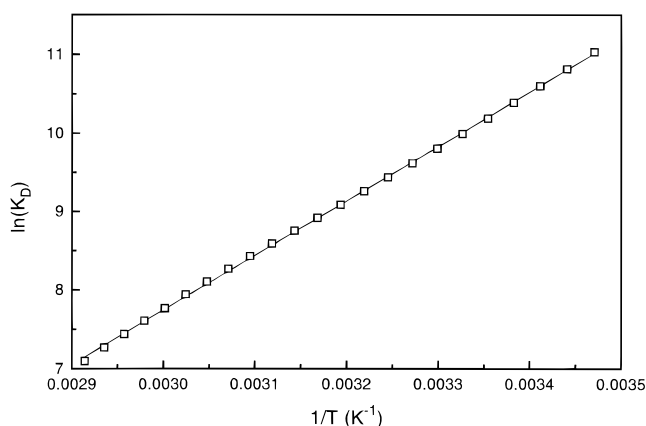


Figure 4. Linear regression of  $\ln K_D$  with respect to  $1/T$ .

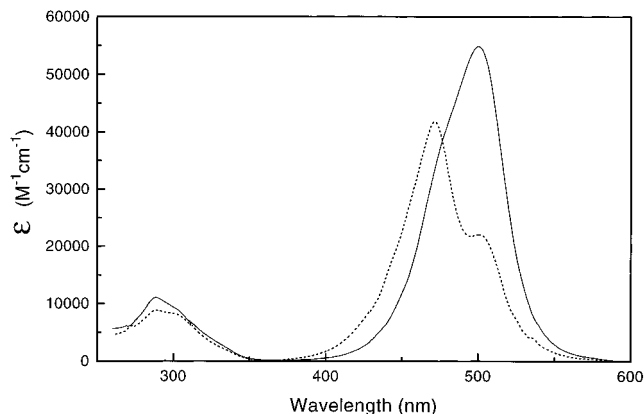


Figure 5. Calculated absorption spectra of the thiazole orange monomer (—) and dimer (- - -).

$$\frac{d \ln K_D(T)}{d(1/T)} = -\Delta H^\circ/R \quad (14)$$

where  $\Delta H^\circ$  is the molar enthalpy change,  $R = 8.31 \text{ J mol}^{-1} \text{ K}^{-1}$  is the universal gas constant, and  $T$  is the Kelvin temperature.  $r_{21}$  can now be determined by requiring that matrix  $\mathbf{R}$  should rotate the target vectors to give concentration vectors (eq 3) that produce an equilibrium constant whose logarithm is a linear function of

(13) Levine, I. N. *Physical Chemistry*, 3rd ed.; McGraw-Hill Book Co.: Singapore, 1988; Section 6.3.

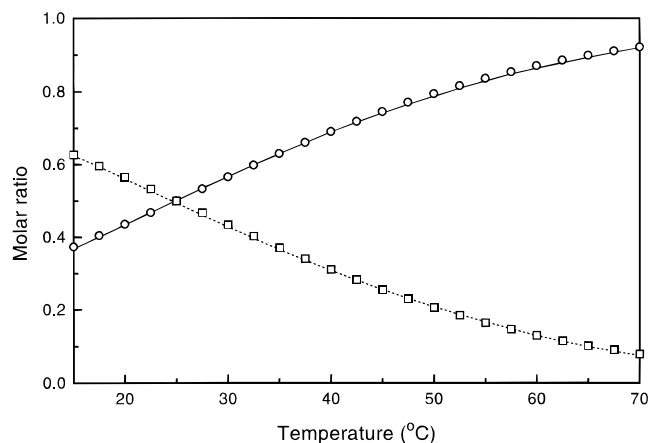


Figure 6. Molar ratios of the thiazole orange monomer,  $c_X/(c_X + 2c_{X_2})$  (○), and dimer,  $2c_{X_2}/(c_X + 2c_{X_2})$  (□), compared to molar ratios predicted by the temperature dependence of the equilibrium constant (shown as lines).

$1/T$ . In practice, the solution is found by a simple search procedure.  $r_{21}$  is given an arbitrary value, for which a trial rotation matrix is calculated (eq 12). This is used to calculate trial concentration profiles (eq 3), which are combined to a trial equilibrium constant (eq 13). A linear regression of the equilibrium constants with respect to  $1/T$  is then performed (eq 14), which determines a trial enthalpy change of the reaction. Each

trial rotation matrix also determines trial spectral responses (eq 4). The procedure is repeated for various values of  $r_{21}$  to find a range that produces reasonable concentration profiles and spectral responses. This is done rather arbitrarily since there is no simple way to estimate  $r_{21}$ . Once a range has been found,  $r_{21}$  is varied gradually in this range, and a  $\chi^2$  (a regression coefficient) is calculated for each regression of  $\ln K_D(T)$  with respect to  $1/T$ . The  $r_{21}$  that produces the best fit determines matrix **R**.

## RESULTS AND DISCUSSION

As a first example, we characterize the dimerization of thiazole orange in aqueous solution. Thiazole orange is a dye that becomes intensively fluorescent upon binding to nucleic acids, making it useful as a DNA staining agent.<sup>14</sup> However, it has been difficult to use thiazole orange for quantitative purposes owing to its propensity to aggregate in aqueous solution. The dye is rather hydrophobic and dimerizes readily. It has also a tendency to adsorb to the walls of its container, which makes it difficult to characterize its dimerization properties by varying the total concentration.<sup>6</sup> By studying the effect of temperature, we use a single sample, which gives us a better control of the adsorption problem. Although adsorption does depend on temperature, the amount of adsorbed dye changed insignificantly within the temperature range studied.

Absorption spectra of thiazole orange were recorded in the temperature range 15–70 °C in 2.5 °C intervals (Figure 1). The

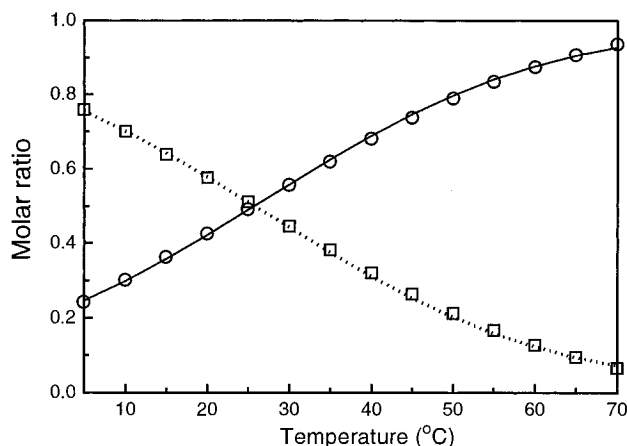
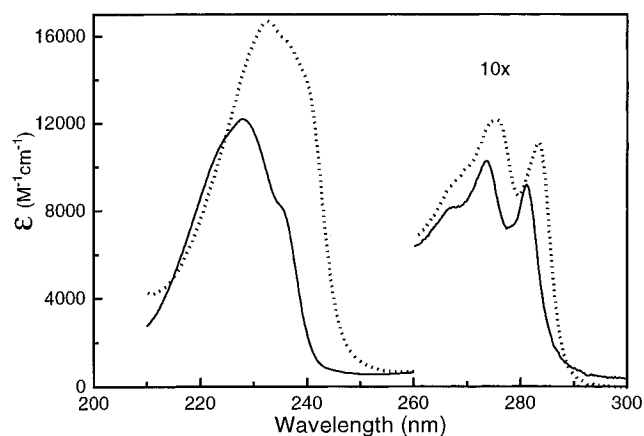
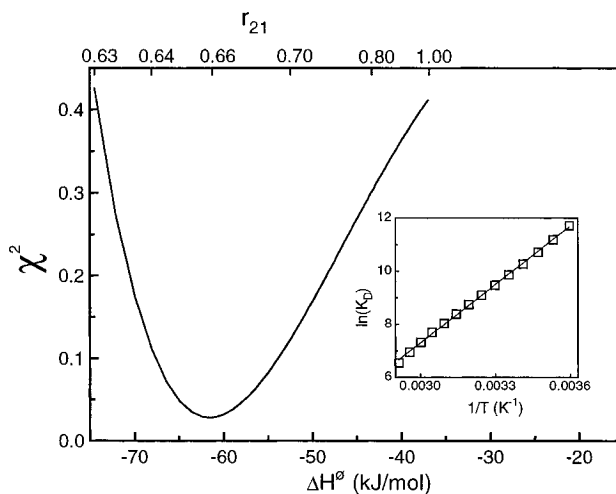
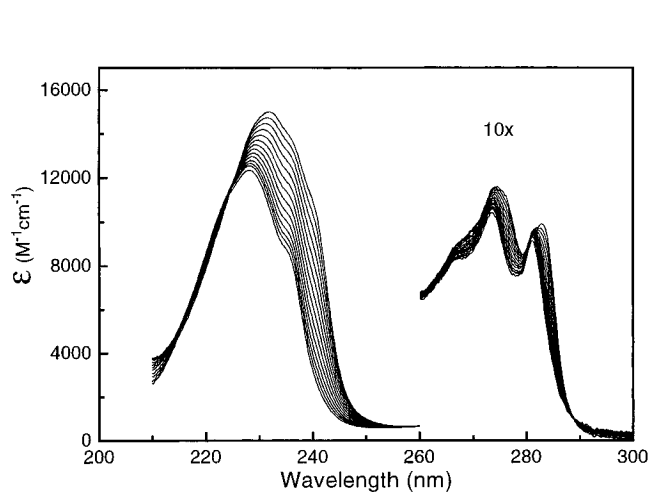


Figure 7. (Top) Left: Absorption spectra of benzoic acid (54  $\mu\text{M}$ ) in *n*-heptane recorded at 5 °C intervals between 5 °C (high intensity) and 70 °C (low intensity). Right:  $\chi^2$  of the linear regression of  $\ln K_D$  with respect to  $1/T$  (inset) as a function of  $\Delta H^\circ$ . (Bottom) Left: Calculated absorption spectra of the benzoic acid monomer (—) and dimer (---). Right: Molar ratios of the benzoic acid monomer,  $c_X/(c_X + 2c_{X_2})$  (○), and dimer,  $2c_{X_2}/(c_X + 2c_{X_2})$  (□), compared to molar ratios predicted by the temperature dependence of the equilibrium constant (shown as lines).

spectra have almost identical intensities at 476 nm, suggesting that this is an isosbestic point that is slightly perturbed due to the temperature dependence of adsorption. Decomposition of the spectra by NIPALS (eq 1) revealed the presence of only two components, supporting this view. These must be the thiazole orange monomer and dimer.

Target and projection vectors were calculated by NIPALS (eq 1), and the target vectors were scaled to add up to the total thiazole orange concentration (Figure 2, top). This defines  $f_{11}$  and  $f_{12}$  (eq 8). A spectrum of the thiazole orange monomer was recorded using a diluted sample ( $18 \mu\text{M}$ ) at  $65^\circ\text{C}$ . It was decomposed into the projection vectors (Figure 2, bottom), determining  $f_{21}$  and  $f_{22}$  (eq 11).

Together  $f_{11}$ ,  $f_{12}$ ,  $f_{21}$ , and  $f_{22}$  define three elements of matrix  $\mathbf{R}$ , leaving only  $r_{21}$  as unknown (eq 12). For various values of  $r_{21}$ , temperature-dependent dimerization constants were calculated, and a linear regression of  $\ln K_D(T)$  with respect to  $1/T$  was performed. The  $r_{21}$  value that produced the fit with lowest  $\chi^2$  was considered correct. In Figure 3, the  $\chi^2$  dependence is shown, both as a function of  $r_{21}$ , which has no immediate physical meaning, and as a function of the associated enthalpy change,  $\Delta H^\circ$ , of the

reaction. Best fit gave  $\Delta H^\circ = -58 \text{ kJ mol}^{-1}$  and  $\Delta S^\circ = -109 \text{ J mol}^{-1} \text{ K}^{-1}$  and generated an almost perfectly linear van't Hoff plot (Figure 4). The spectral profiles and concentrations corresponding to this solution are shown in Figures 5 and 6. As a second example, we characterize the benzoic acid monomer/dimer equilibrium in *n*-heptane (Figure 7). We obtain  $\Delta H^\circ = -61 \text{ kJ mol}^{-1}$  and  $\Delta S^\circ = -123 \text{ J mol}^{-1} \text{ K}^{-1}$ . This corresponds to  $K_D = 13.2 \times 10^3 \text{ M}^{-1}$  at  $30^\circ\text{C}$ , which is in good agreement with previous determinations of  $15.9 \times 10^3$  and  $8.7 \times 10^3 \text{ M}^{-1}$ .<sup>6,8</sup>

#### ACKNOWLEDGMENT

This work was supported by the Swedish Research Council for Engineering Sciences. The government of Galicia (Xunta de Galicia, Spain) is acknowledged for a grant supporting the visit of J.M.A in Göteborg.

Received for review November 27, 1995. Accepted March 1, 1996.<sup>⊗</sup>

AC951147P

---

(14) Kienast, J.; Schmitz, G. *Blood* **1990**, 75, 116–121.

---

<sup>⊗</sup> Abstract published in *Advance ACS Abstracts*, April 1, 1996.